

A novel concept for the detection of tau neutrino appearance

Roger Forty

CERN, Geneva

E-mail: Roger.Forty@cern.ch

ABSTRACT: A novel concept for the detection of tau neutrinos is presented, potentially suitable for use in a long-baseline neutrino oscillation experiment. It relies on the direct identification of the tau leptons produced in charged-current interactions, by imaging the Cherenkov light that the tau generates in C_6F_{14} liquid. In a simple simulation about half of the tau leptons can be successfully identified in this way.

KEYWORDS: Neutrino Detectors and Telescopes.

Contents

1. Introduction	1
2. Detector concept	2
3. Possible implementation	7
4. Conclusions	9

1. Introduction

Strong evidence for neutrino oscillation has come from SUPER-KAMIOKANDE, from the zenith angle dependence of the muon deficit that they observe for atmospheric neutrinos [1]. The favoured explanation is the oscillation of muon neutrinos to tau neutrinos, which escape detection in their apparatus. These results require confirmation using an artificially generated neutrino beam, and accelerator-based experiments that will check the muon neutrino disappearance are underway [2, 3]. A long-baseline beam from CERN to Gran Sasso is also under discussion [4]. As the question of ν_μ disappearance should have been settled by the time that experiments using that beam take data, the key issue for them is to confirm that tau neutrinos are indeed being produced. Since the neutral current interactions of the ν_τ cannot be distinguished from those of other neutrinos, the crucial point is to identify charged-current interactions, $\nu_\tau N \rightarrow \tau^- X$, by the appearance of the tau lepton.

Two experiments are being proposed to make this measurement: OPERA [5] and ICANOE [6]. OPERA seeks to identify the taus by their characteristic short lifetime, corresponding to an average decay length of about 1 mm for the CNGS beam energy spectrum. They propose to use an emulsion target to recognise the kink from the tau decay, building on the expertise accumulated by the CHORUS [7] and DONUT [8] experiments. ICANOE, on the other hand, intends to recognise the charged-current ν_τ events through kinematical criteria, involving the missing energy from the neutrinos accompanying the tau decay, and isolation criteria for the tau decay products, following the approach pioneered by NOMAD [9]. These experiments will be challenging, as the number of charged-current ν_τ interactions expected in each year of operation of the CNGS beam is only about 30 per kiloton of sensitive detector mass [4], for the oscillation parameters preferred by the SUPER-KAMIOKANDE data: $\Delta m^2 = 3.5 \times 10^{-3} \text{ eV}^2$, $\sin^2(2\theta) = 1$ [10]. Maintaining high

efficiency is therefore crucial, whilst background must be suppressed such that just a few observed events would correspond to an unambiguous signal.

The detection technique presented in this note is different — the idea is to directly identify the tau by imaging the Cherenkov light that it produces. Cherenkov detectors have already been used in this field: SUPER-KAMIOKANDE itself relies on the generation of Cherenkov light in water, but without focussing. A ring-imaging water Cherenkov detector, AQUA-RICH [11], was originally proposed for Gran Sasso, but insufficient sensitive mass could fit in the experimental halls, so it is now being pursued as an atmospheric neutrino experiment sited elsewhere (with a megaton mass!). Due to the chromatic dispersion in water, a relatively narrow energy bandwidth is assumed for photon detection in AQUA-RICH. Coupled with the 20% detector coverage this leads to typically 0.5 detected photons per mm of track length, insufficient to see the tau track. The concept presented here is to use C_6F_{14} liquid as the radiator, which due to its low dispersion allows a wider photon energy bandwidth, and to have full detector coverage. This leads to 13 detected photons per mm, and direct detection of the Cherenkov ring from the tau then becomes feasible. Furthermore, the increased density of the radiator would allow a kiloton detector to fit comfortably in a Gran Sasso hall.

2. Detector concept

Perfluorohexane (C_6F_{14}) is a well-established radiator material for RICH detectors [12, 13], liquid at room temperature. About a ton of it is used in DELPHI [14]. It has the nice features for this application of a refractive index of about 1.27, slightly lower than that of water, whilst being significantly more dense (1.68 g/cm^3). It is also, after purification, highly transparent to photons with wavelength down to 200 nm and beyond [14], and has low chromatic dispersion: the dependence of the refractive index on photon energy is shown in figure 1a.

A classical focussed RICH geometry is adopted, with a spherical mirror following the radiator and a spherical detection surface sited at radius

$$r_d = \frac{r_m}{2} \frac{\sqrt{1 + \frac{9}{16} \sin^2 \theta_c + \frac{3}{8} \sin^2 \theta_c}}{1 - \frac{3}{16} \sin^2 \theta_c}, \quad (2.1)$$

where r_m is the mirror radius of curvature and θ_c is the Cherenkov angle [16]. The saturated Cherenkov angle in C_6F_{14} is about 38° , and so $r_d = 0.67 r_m$.

The tau leptons produced by charged-current interaction of neutrinos from the CNGS beam are produced in the predominantly forward direction, along the direction of the beam. The detector elements are therefore oriented to collect the light produced by such tracks, as shown schematically in figure 2a. The assumed quantum efficiency $Q(E)$ of the photodetectors is shown in figure 1b; it is cut off above 6.2 eV,

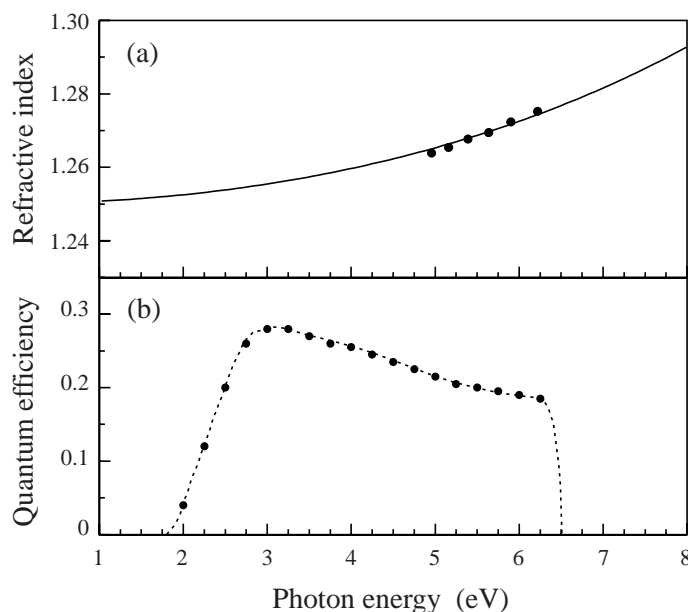


Figure 1: (a) Refractive index versus photon energy for C_6F_{14} liquid: the points are data taken from [15], with a superimposed single-pole Sellmeier form, adjusted to agree with unpublished data in the visible. (b) Assumed quantum efficiency versus photon energy for the photodetector: the points are taken from a Hamamatsu specification for a bialkali photocathode.

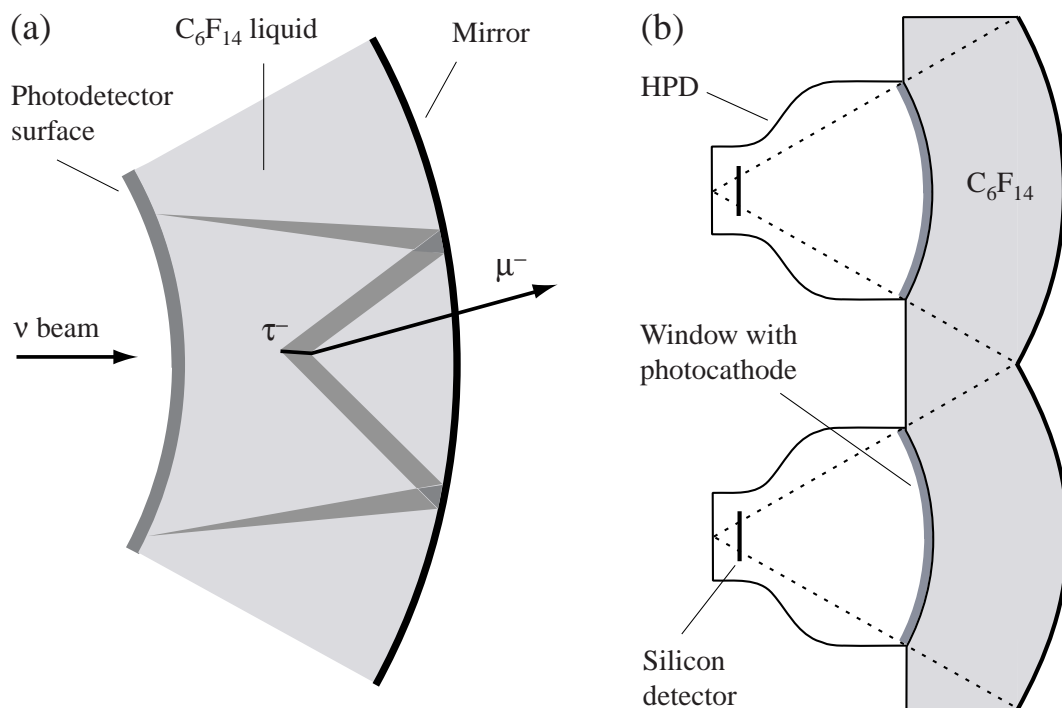


Figure 2: (a) Schematic layout of a detector module; the focussing of the Cherenkov light emitted by the tau is indicated. (b) A possible implementation using large HPDs as the photodetectors.

corresponding to a quartz entrance window for the detectors. The possible implementation of this concept illustrated in figure 2b will be discussed in the following section. For the purposes of the simulation presented here, a circular detector surface of 1 m diameter is assumed, equal to its radius of curvature. The radiator thickness is then 50 cm, with a spherical mirror of radius 150 cm. Such a module would contain about 0.67 m^3 of C_6F_{14} liquid, corresponding to about 1100 kg. A kiloton detector would thus require about 900 such modules.

Cherenkov photons produced by the tau and other charged particles in the event are focussed by the mirror into rings on the detector surface. For full detector coverage, the number of detected photoelectrons per ring is given by:

$$N = \left(\frac{\alpha}{\hbar c} \right) L \int QTR \sin^2 \theta_c dE, \quad (2.2)$$

where the factor in parentheses is a constant with value $370 \text{ eV}^{-1} \text{ cm}^{-1}$, L is the track length in the radiator, T is the transmittance of the radiator, and R is the reflectivity of the mirror (assumed to be 95%) [16]. The absorption length of purified C_6F_{14} has been measured to be greater than 100 cm for $E < 6.2 \text{ eV}$ [17], so $T = 1$ is assumed here. Then eq. (2.2) corresponds to 13 detected photoelectrons per mm of track length, which renders the tau track visible. The muon from $\tau^- \rightarrow \mu^- \nu_\tau \bar{\nu}_\mu$ decays will typically pass through 25 cm of radiator, giving 3200 photoelectrons. The RICH optics result in the position of the rings on the detector surface being determined by the angle of the tracks, insensitive to their production point in the radiator, and is thus well adapted to identification of the tau decay kink.

Such events have been simulated, taking the tau and muon track parameters from a detailed simulation of quasielastic interactions of a neutrino beam with the CNGS energy spectrum [18]. In quasielastic events $\nu_\tau n \rightarrow \tau^- p$ the only other track is a proton, which is below threshold for producing Cherenkov light if it has momentum less than 1.2 GeV: this is the case for 85% of the simulated events. For this simple simulation, multiple scattering of the tracks was ignored, and photons generated along the track length in the radiator according to the distribution shown in figure 1b, calculating their Cherenkov angle according to the dispersion curve in figure 1a. A typical event is shown in figure 3a, where the tau decay length was 1.5 mm and the kink between tau and muon was 100 mrad. The signature of such decays will thus be a densely populated ring from the muon, accompanied by an offset low-intensity ring from the tau. In the case of $\tau^- \rightarrow e^- \nu_\tau \bar{\nu}_e$ decays, the electron will shower in the C_6F_{14} , giving a more diffuse ring than for the muon, making the separation of the tau hits more difficult. For the single-prong hadronic decay (corresponding to about half of the tau decays) there is a high probability of the hadron escaping without nuclear interaction: for the radiator interaction length of about 55 cm, a hadronic track of 25 cm length has 63% probability of not interacting; these events may therefore also be useful.

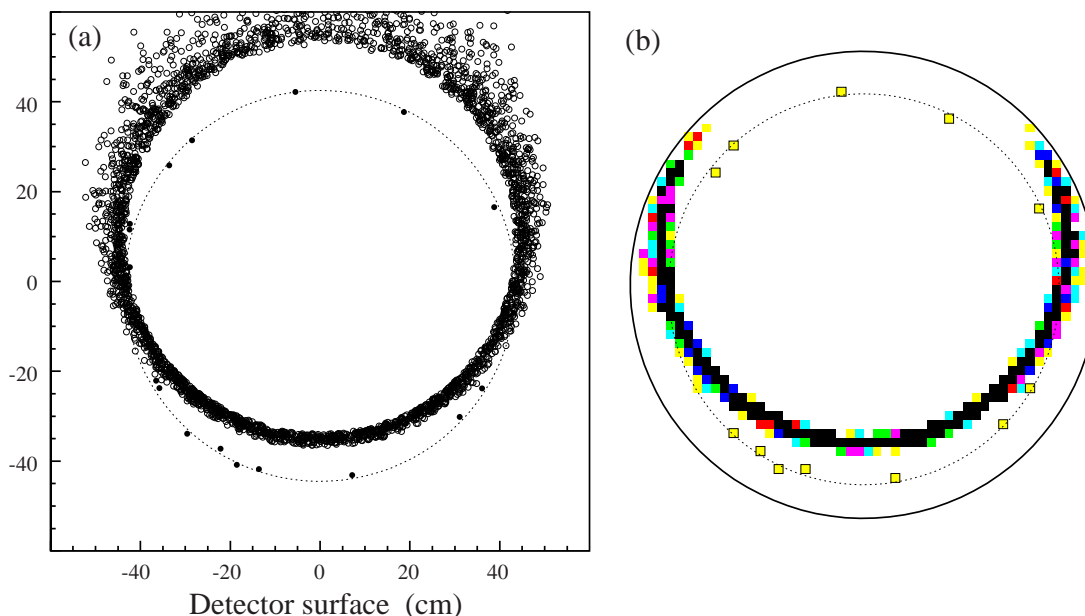


Figure 3: Display of a single $\tau^- \rightarrow \mu^- \nu_\tau \bar{\nu}_\mu$ event in the detector module: (a) impact points of the detected photoelectrons on the detector surface; those from the tau are marked with solid points, with the ring image indicated by a dashed line. (b) The same event after pixellization of the detector surface (within a radius of 50 cm); the density of shading increases with increasing number of detected photoelectrons.

The angular distribution of the tau tracks relative to the incoming neutrino direction in the simulated events is shown as the solid line in figure 4a; as can be seen it is strongly peaked in the forward direction, with a mean of only 40 mrad, whilst the distribution of the kink angle between the tau and muon tracks is broader (dashed in the figure) with a mean of 150 mrad. The momentum distribution of the taus is shown in figure 4b: all are above the threshold for generating Cherenkov light, which is 2.3 GeV for the tau in C_6F_{14} . The distribution of the number of detected photoelectrons from the tau track is shown in figure 4c. About 60% of the events have 6 or more detected hits, which should be sufficient to recognize the ring.

The selection of tau events can use not only the signature of the offset low-intensity ring, but also the measurement of the average Cherenkov angle of the associated photons. For this, good resolution is required to positively identify the tau by separating its ring radius from that expected for a saturated track (as would be the case for lighter particles: e , μ or π), as well as to distinguish the photons from different tracks. A tau with the typical momentum of 20 GeV emits Cherenkov light at an angle which is 5 mrad less than a fully relativistic particle.

The Cherenkov angle resolution due to dispersion in the radiator has an RMS of 10 mrad per photoelectron, corresponding to 0.7 cm on the detector surface. A detector granularity of $2 \times 2 \text{ cm}^2$ is therefore suitable, to avoid limiting the resolution.

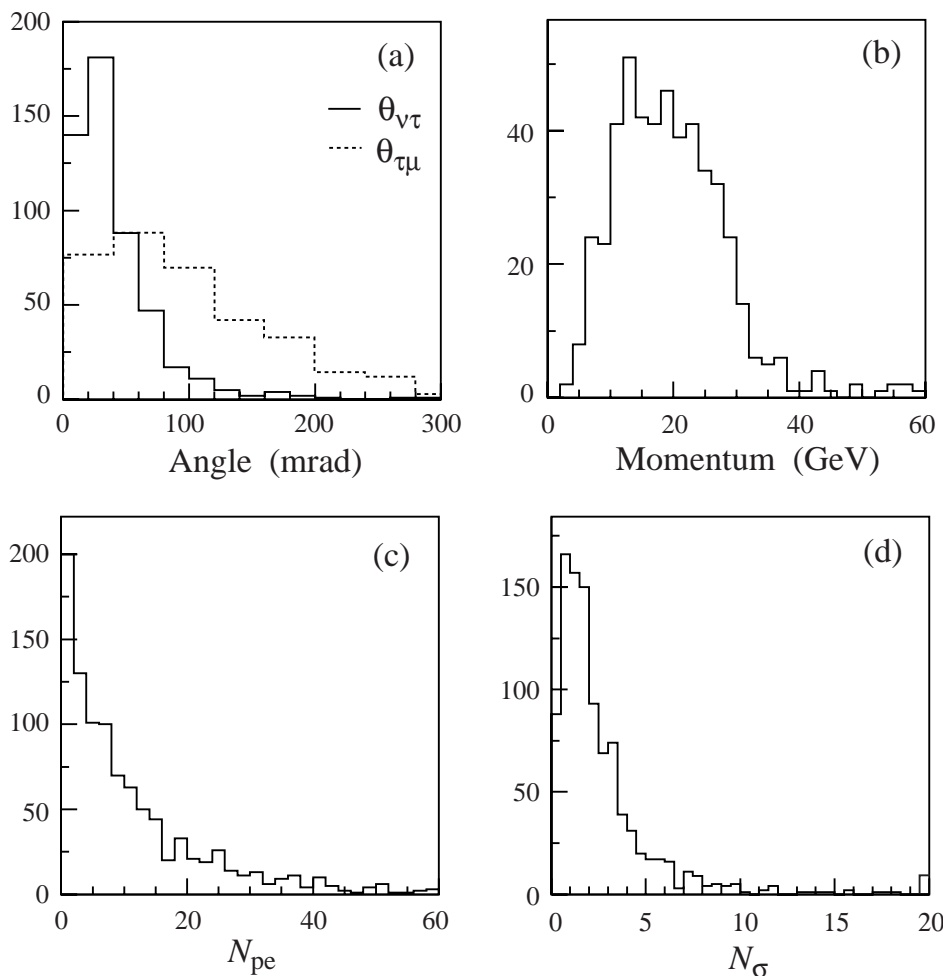


Figure 4: Distributions from simulated tau neutrino interactions: (a) angular distributions of the tau (solid) and muon (dashed), (b) tau momentum, (c) number of detected photoelectrons from the tau, (d) significance of the difference between the tau hypothesis and the saturated Cherenkov angle, for the tau track.

Because of its short decay length, there is no smearing due to emission-point uncertainty for photons from the tau. For longer tracks, such as the muon in figure 3a, there is noticeable effect from spherical aberration, leading to a tail of photons on the outside of the ring; this, however, tends to be on the side away from the tau ring, and so should not degrade the pattern recognition. The result of pixellization of the detector plane is shown for the same event in figure 3b.

The determination of the production point of the tau can be achieved by localizing the muon track as it leaves the detector module, using a tracking detector. The Cherenkov ring of the muon gives a very precise measurement of its angle, and the integrated number of photoelectrons detected on the ring is proportional to the path length. The tau production point should be localized in this way to a precision in space of order 1 cm, more than adequate for the Cherenkov angle calculation.

The average Cherenkov angle is determined for all photons from the tau in each event, and compared to the value expected for a saturated ring. The significance of the separation, expressed as the number of sigma N_σ between the tau hypothesis and the saturated Cherenkov angle, is shown in figure 4d. Of course, the tau momentum is not fully reconstructed; nevertheless, the measured muon momentum will provide a lower limit on the tau momentum, and for the typical muon momenta observed all light particle types would give a saturated ring. About half of the tau tracks have significant separation ($N_\sigma > 2$), with 30% having $N_\sigma > 3$. The significance could be increased by improving the resolution with a narrower bandwidth of photon energies, at the cost of reducing the total number of photoelectrons observed; the optimal cut will depend on the level of background that needs to be rejected. The performance will also be reduced somewhat due to confusion with overlapping rings from other tracks in the event. In particular, for the muon decays, a kink angle greater than about 40 mrad will be required to separate the tau and muon images; this occurs in about 80% of events. Detailed study of the loss due to pattern recognition awaits a more complete simulation of the events.

3. Possible implementation

To keep high detection efficiency it is advantageous to cover the detection surface of a module with a single detector. Since the mass of radiator that is imaged by a detector scales as the cube of the detector diameter, the largest possible detectors are desirable to limit the number required. A 1 m diameter hybrid photodiode (HPD) detector has been proposed for AQUA-RICH [11]. These devices combine the photocathode and focussing of vacuum photodetectors with the spatial and energy resolution of silicon detectors. They have been the subject of an intense program of R&D for the RICH detectors of the LHCb experiment [19, 20], and one of the devices developed has 2048 channels in a 5" diameter (127 mm) envelope [21]. These tubes are fabricated at CERN with a bialkali (K_2CsSb) photocathode.¹ A recent test-beam image from one of them is shown in figure 5a. Envelopes for a 10" version of this tube have recently been manufactured, and a 20" version is already foreseen (the photomultipliers used by SUPER-KAMIOKANDE are also of 20" diameter). Extrapolation to a 40" (1 m) diameter tube appears feasible. With 2048 channels, the effective pixel size at the photocathode would be $2 \times 2 \text{ cm}^2$, ideal for the present application. The excellent energy resolution makes photon counting straightforward in these tubes, as illustrated in figure 5b.

¹Note that Hamamatsu is advertising an HPD with GaAsP photocathode that achieves 45% quantum efficiency at 500 nm: such performance could double the number of detected photoelectrons from the tau.

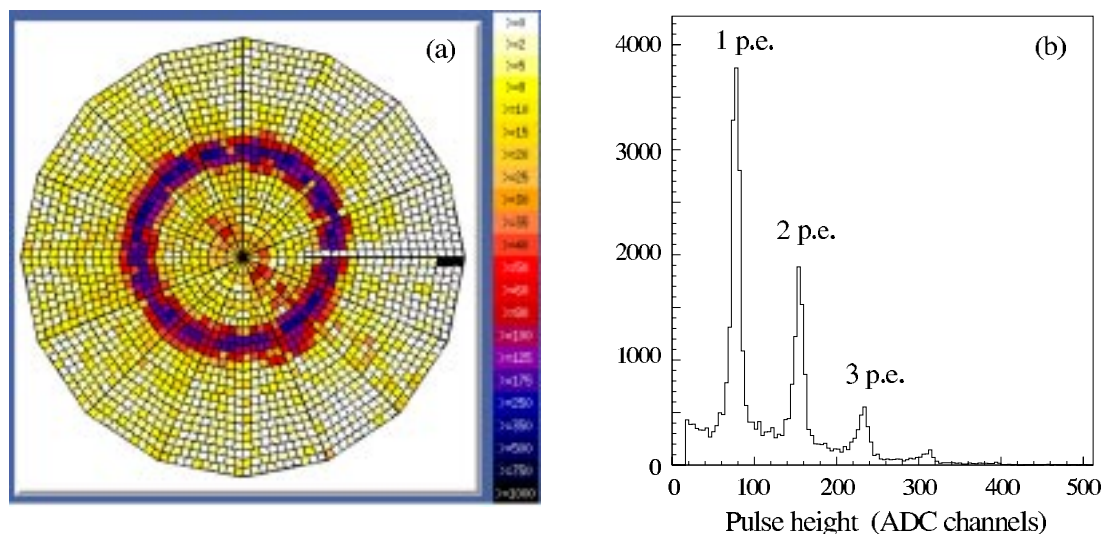


Figure 5: (a) Display of beam-test data in the 2048-pad HPD, showing the accumulated ring image produced by a pion beam passing through a gas radiator; (b) pulse-height spectrum from an HPD, showing the well-separated photoelectron peaks.

With such an HPD as the photodetector, the layout of a module would be as shown in figure 2b. Neighbouring modules would be connected so that their radiators fill a single volume. Modules could be stacked vertically, with hexagonal close packing, to make a wall. Each wall would then be followed by a tracking station, and this structure repeated as often as necessary to provide the detector mass required. Sixteen walls, each of 61 modules, would provide a kiloton mass, as illustrated in figure 6a. Interleaving of toroidal magnets would allow the muon momentum and charge to be determined. The first tracking station would act as a veto against charged particles entering the apparatus from upstream, whilst the last station is separated by sufficient lever arm to provide a measurement of the track angle after the last magnet. The required number of magnet and tracking stations would clearly be a matter for detailed optimisation.

A more compact detector would be possible if a radiator of higher density was available. However, other possibilities that have been investigated such as lead glass, whilst being suitably dense, also have a much higher refractive index, so the volume imaged per detector is reduced (by eq. (2.1)). Furthermore they lack the low chromatic error and large photon bandwidth of C_6F_{14} . Nevertheless, a suitable glass may still be found.

If the use of individual detectors for each module is abandoned, then the module size could increase. The extreme case would be a large volume of radiator limited by the dimensions of the experimental hall: for example, a spherical mirror of radius 9m with a radiator length of 3m and an array of detectors covering the upstream surface. The photodetector coverage would be a little lower, due to the packing of

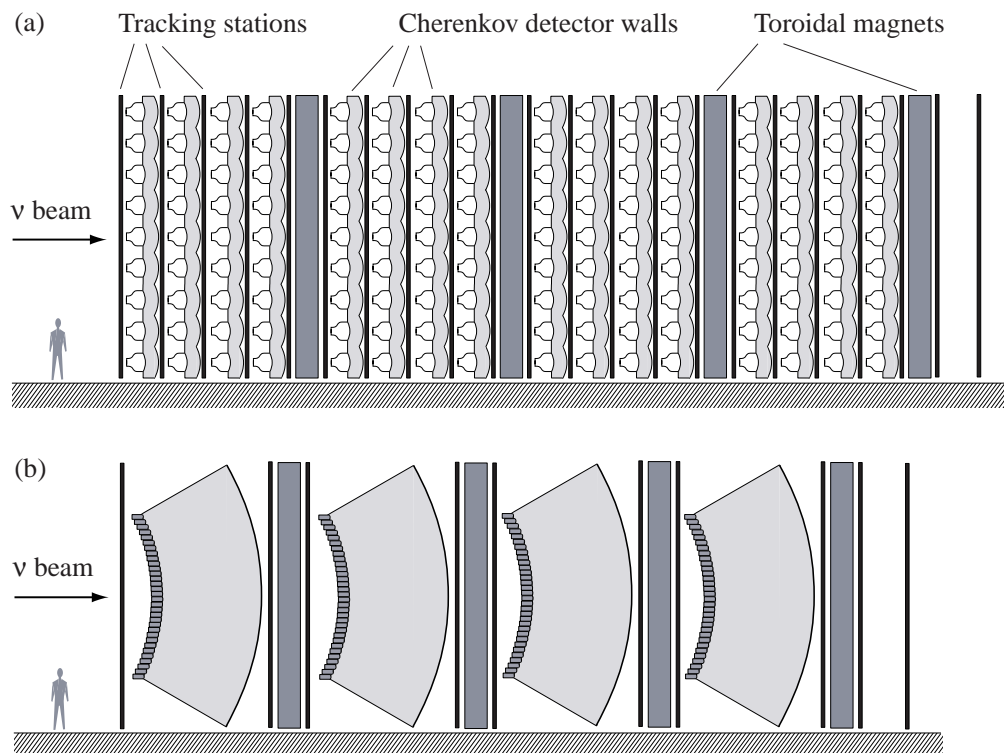


Figure 6: Two possible layouts of detector modules to form a kiloton experiment: (a) using large HPDs for the photodetector, (b) covering the detection surface with many close-packed tubes.

the tubes, and the transparency of C_6F_{14} over such a long radiator length would need to be studied. Also the large number of photons from a muon track would give strong constraints on the mirror quality, to avoid a tail of poorly reflected photons obscuring the tau signal. The advantages are the significantly reduced number of channels required, and the possibility of using standard photodetectors. One such module would have a radiator mass of 240 t, so could replace a series of four walls of modules in the previous layout, as illustrated in figure 6b. The optimal choice may lie somewhere between these two limits.

4. Conclusions

A novel concept for detection of tau neutrinos has been presented, through their charged-current interaction in C_6F_{14} liquid to give a tau lepton, that produces sufficient Cherenkov light for a ring image to be formed. The signature, for $\tau \rightarrow \mu$ decays, is of a densely populated ring from the muon, accompanied by an offset low intensity ring from the tau. In about half of the events in a simple simulation a positive identification of the tau can be achieved through the measurement of the average Cherenkov angle of the detected photons.

The expected number of events passing the selection cuts for a kiloton detector in the CNGS beam can be estimated as follows. For the oscillation parameters preferred by SUPER-KAMIOKANDE data about 30 charged-current ν_τ interactions would be expected per year. Assuming that $\tau \rightarrow \mu$ and single-prong hadronic decays are usable, the branching fraction is 67%. Requiring enough detected photoelectrons to recognize the tau ring, and sufficient kink of the decay product to give well separated rings, bring efficiency factors of 60% and 80% respectively. The efficiency loss due to pattern recognition when there are other tracks in the event (for example, from nuclear breakup in deep-inelastic interactions) or from hadronic reinteraction has not yet been studied. Allowing a factor of two for such effects, there would still be about 5 detected signal events per year (or 20 from a four-year run). The key issue will then be the expected background.

A potential source of background that remains to be quantified is the production of knock-on electrons from the tau decay track. These will produce Cherenkov light if above 0.6 MeV. Their contribution to the background will only be significant if they lie outside the angular cut of 40 mrad from their parent track that was applied above. Other background sources need to be addressed, including the effect of mirror imperfections, and backscattering from the silicon of the HPD. They could also be studied with a small-scale beam test. If the background is found to be significant, then a further cut could be applied on the Cherenkov ring radius, to positively identify the tau: this should suppress all background, but with the corresponding reduction in efficiency that was discussed earlier. Clearly the next step would be a detailed simulation of all tau-neutrino interactions in the detector; the purpose of this note is to gauge the interest in the detector concept, before embarking on such a programme.

Acknowledgements

It is a pleasure to thank Tom Ypsilantis for inspiration and advice: he suggested the use of C_6F_{14} as radiator, and pointed me to eq. (2.1). Thanks also to Ioannis Papadopoulos and Pietro Antonioli, who provided the simulated events used here, and to Christian Joram for the HPD information.

References

- [1] SUPER-KAMIOKANDE collaboration, Y. Fukuda et al., *Evidence for oscillation of atmospheric neutrinos*, *Phys. Rev. Lett.* **81** (1998) 1562 [[hep-ex/9807003](#)].
- [2] K2K collaboration: <http://neutrino.kek.jp>.
- [3] MINOS collaboration, Technical Design Report, NuMI-L-337 (October 1998), <http://www.hep.anl.gov/NDK/Hypertext>.

- [4] R. Bailey et al., *The CERN neutrino beam to Gran Sasso (NGS)*, CERN-SL/99-034, INFN/AE-99/05.
- [5] OPERA collaboration, *A long baseline ν_τ appearance experiment in the CNGS beam*, CERN/SPSC 99-20 (August 1999).
- [6] ICANOE collaboration, *A proposal for a CERN-GS long baseline and atmospheric neutrino oscillation experiment*, CERN/SPSC 99-25 (August 1999).
- [7] CHORUS collaboration, E. Eskut et al., *The CHORUS experiment to search for $\nu_\mu \rightarrow \nu_\tau$ oscillation*, *Nucl. Instrum. Meth.* **A 401** (1997) 7.
- [8] E872 collaboration, *E872: the direct observation of the ν_τ* , *Nucl. Phys.* **70** (Proc. Suppl.) (1999) 204.
- [9] NOMAD collaboration, *The NOMAD experiment at the CERN SPS*, *Nucl. Instrum. Meth.* **A 404** (1998) 96.
- [10] C. Walter, *Results from SUPER-KAMIOKANDE and the status of K2K*, presentation at Int. Conf. HEP99, Tampere (July 1999).
- [11] AQUA-RICH collaboration, P. Antonioli et al., *Nucl. Instrum. Meth.* **A 433** (1999) 104.
- [12] DELPHI collaboration, *The barrel ring imaging Cherenkov counter of DELPHI*, *Nucl. Instrum. Meth.* **A 323** (1992) 351;
W. Adam et al., *The forward ring imaging Cherenkov detector of DELPHI*, *Nucl. Instrum. Meth.* **A 338** (1994) 284.
- [13] SLD collaboration, *Performance of the Crid at SLD*, *Nucl. Instrum. Meth.* **A 343** (1994) 74.
- [14] E. Albrecht et al., *Nucl. Instrum. Meth.* **A 433** (1999) 47.
- [15] J. Seguinot et al., CERN-EP/89-92 (July 1989).
- [16] T. Ypsilantis and J. Seguinot, *Theory of ring imaging Cherenkov counters*, *Nucl. Instrum. Meth.* **A 343** (1994) 30.
- [17] R. Arnold et al., *A ring imaging Cherenkov detector: the DELPHI barrel rich prototype. Part B: experimental studies of the detector performance for particle identification*, *Nucl. Instrum. Meth.* **A 270** (1988) 289.
- [18] P. Antonioli, private communication, October 1999.
- [19] LHCb collaboration, *A large hadron collider beauty experiment for precision measurements of CP violation and rare decays*, CERN/LHCC 98-4 (February 1998).
- [20] E. Albrecht et al., *Performance of hybrid photodetector prototypes with 80% active area for the RICH counters of LHCb*, presentation at 2nd Conf. on New Develop. in Photodet., Beaune (June 1999).
- [21] A. Braem et al., *Large-area hybrid photodiodes with enclosed VLSI readout electronics*, presentation at 2nd Conf. on New Develop. in Photodet., Beaune (June 1999).